On the inter-ring torsion potential of regioregular P3HT: a first principles reexamination with explicit side chains†

Alberto Baggioli and Antonino Famulari*

Received 6th November 2013,
Accepted 7th December 2013

Introduction

A large part of the modern technologies relies not only on the classic inorganic materials but also on advanced organic molecular systems. The latter are generally based on conjugated molecules, oligomers and polymers, whose applications are allowed by the compatibility with low temperature processing, relatively simple thin-film device fabrication, and the ability to fine-tune their electronic properties by synthetic means.[1] In particular, organic semiconducting materials proved to be suitable for sensible applications in the field of opto-electronics[2] and photovoltaics.[3] In the latter case, bulk hetero-junction devices based on poly(3-alkylthiophenes) (P3ATs) and fullerene derivatives are among the most promising performance-wise and the most extensively investigated from both the experimental and the theoretical points of view.[4] However, among the open issues in the field of conjugated polymer-based materials is that of the so called *side chains*, covalently-attached appendages used to impart suitable mechanical properties to the polymer chains. P3ATs and other alkylthiophene-based copolymers are no exceptions. Alkyl side chains, in particular, are known to improve solubility in organic solvents and to prevent tight packing of large aromatic fragments.[5]

It has been shown that the regioregularity of P3AT polymer chains (*i.e.*, the percentage of head-to-tail linkages between monosubstituted monomer units in the polymer backbone) affects the morphology of the films and their electronic properties.[6] It is generally accepted that the low compatibility between the conjugated polythiophene backbone and alkyl side chains results in a lamellar ''self-assembled'' structure in which π-stacked polythiophene backbones alternate with layers of more or less ordered alkyl fragments.[7–10] Although size and orientation of the crystalline domains can be influenced by the preparation method employed (such as spin-coating, dip-coating, drop-casting, direct epitaxial crystallization),[11] P3ATs form semicrystalline films in which the crystalline domains are dispersed into an amorphous matrix. The power conversion efficiency of devices based on such thin films is related to the formation of the charge carriers at the donor/acceptor interface, and to the charge carrier migration toward the electrodes.[12] The latter charge transport process depends only marginally on the mobility along conjugated polymer chains within the crystalline domains, and is substantially determined by the transport capabilities of the disordered interlamellar regions.[13] While a complete understanding of

Dipartimento di Chimica, Materiali e Ingegneria Chimica ''G. Natta'', Politecnico di Milano, via Mancinelli 7, I-20131 Milano, Italy. E-mail: alberto.baggioli@polimi.it, antonino.famulari@polimi.it

† Electronic supplementary information (ESI) available: Optimized structures of all conformational isomers of HBT discussed are provided in the Cartesian format.

specific inter-chain interactions within such morphologies is essential to the performance-tailoring of these materials, large-scale heterogeneity and overall complexity are major obstacles to the investigation of these systems, as bulk methods characterize only average properties. In order to gain useful insights into the underlying mechanisms, synergistic experimental and theoretical studies are mandatory. However, computational modelling of realistically large-sized systems may be impractical for many reasons.[14,15]

The most pressing concern when trying to simulate a physical process is usually that of the very *size* of the system to be treated. This is because the minimum scale at which the majority of technologically-relevant physical processes take place lies well beyond the reach of currently available highly-accurate wavefunction-based computational methods.[16] A certain degree of approximation is thus unavoidable, ranging from the density functional theory formalism (DFT methods),[17] to the neglect of diatomic differential overlap formalism (NDDO-based algorithms such as AM1[18] and PM*n*[19] semiempirical quantum mechanical methods),[20] to molecular mechanics force fields parameterized either on experimental or computational reference data.[21] The inexpensiveness of such approximate theoretical models, compared to more rigorous *ab initio* quantum chemical approaches like the coupled cluster theory,[22] comes with a price in terms of accuracy and reliability. The number of empirical parameters introduced, together with the severity of the approximations employed, may result in unreasonably large uncertainties in the calculations.[21] As a matter of fact, whereas the affordability of a computational method is vital in order to allow the simulation of large-scale molecular systems, consistency with reference data (either experimental or from higher-level calculations) is to be ensured in order to assess the reliability of the said computational approach.

Due to mainly technological constraints, medium to large systems[23] are usually modelled by molecular mechanics (MM) means through a suitably parameterized force field, either at atomistic or coarse grained level.[24] The total energy of a molecular cluster described at such levels of theory is represented by a summation of classical potentials (*e.g.* Coulomb and Lennard-Jones potentials), whose parameters are fitted on a selection of reference data, commonly obtained at the quantum mechanical (QM) level on small representative molecular systems.[21,24] The ability to provide accurate predictions on fundamental and non-trivial subjects of general interest is in fact at the basis of the great attention paid nowadays to accurate *ab initio* quantum chemical approaches, overshadowing their general expensiveness and steep scaling with increasing size of the target systems.[21,24]

Although it is now known that alkyl side chains exert a non-negligible effect on the morphological motifs of P3ATs for thin film applications,[8f,11a] molecular dynamics simulation on the bulk of such materials typically makes use of all-purpose force fields which lack the specificity needed for an accurate description of certain phenomena.[25] A few attempts at the production of *ad hoc* force fields have been reported lately,[26] but several *a priori* assumptions are still made in order to simplify the process of harvesting reference data from QM calculations. In particular, it is common to shorten or completely remove alkyl substituents in the calculation of inter-ring torsion potentials, as the former is assumed to adopt a staggered extended conformation such as that expected from linear alkanes in the gas phase. On this matter, the authors recently reported for the 3-hexylthiophene monomer the existence of non-extended side chain conformations accessible at around room temperature and compatible with P3AT known packing motifs.[27]

The aim of this present report is to contribute to the collective pursuit of an optimal force field parameterization for P3ATs and other alkylthiophene-based polymers and oligomers, by providing accurate inter-ring torsion potentials through explicit treatment of the alkyl side chain at its full length. The conformational problem of a monosubstituted bithiophene molecule is tackled at the Møller–Plesset second-order perturbation theory (MP2)[28] level with a triple-ζ split-valence basis set with polarization functions on all nuclei.[29] In particular, this study will provide a number of minimum energy conformations suitable as building blocks for alkylthiophene-based atomistic models, including a few energetically-favourable cases featuring a cisoid inter-ring arrangement, which may shed new light on the controversial subject of chain-folding in P3ATs and other poly(alkylthiophene) derivatives.

Theoretical methods

For the task of simulating a regioregular poly(3-hexylthiophene) (P3HT) chain segment, 3-hexyl-2,2′-bithiophene (HBT) was chosen. Calculations on HBT were carried out at the all-electrons MP2/6-311G(d,p) level using the Gaussian 09 suite of programs.[28–30] The conformational problem of this monosubstituted bithiophene is studied by considering three dihedral angles, the inter-ring angle θ and the first two angles of the side chain α and β, as shown in Fig. 1. Methodology and part of the nomenclature for this investigation mimic those already employed for the 3-hexylthiophene monomer in a previous report.[27] Torsion potential energy curves were generated through a series of constrained geometry optimizations, in which one dihedral angle at a time was incremented in steps of 1–3°, relaxing all other geometrical parameters. Dihedral angles of the side chain beyond β were initially set to all-staggered configuration compatibly with P3AT packing requirements. No attempt was made in order to evaluate the basis set superposition error (BSSE)[31] contribution to the reported MP2

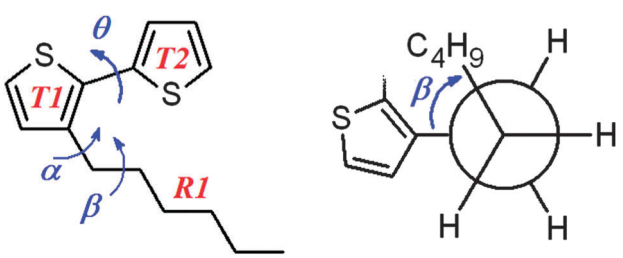

Fig. 1 Naming of the different fragments of 3-hexyl-2,2′-bithiophene for ease of discussion, and definition of θ, α and β angles.

energies, but it was shown[27] that it is roughly equivalent between *anti* and *gauche* side chain arrangements of 3-hexylthiophene, and we expect this phenomenon to hold true also in the case of 3-hexyl-2,2′-bithiophene.

A monosubstituted bithiophene molecule was used in place of an actual head-to-tail P3HT dimer because an additional alkyl chain R2 on T2 would not extend toward T1, nor toward R1. The interactions of a second side chain with T1 and R1 are thus considered negligible in this study. Moreover, the $\{\theta, \alpha, \beta\}$ tern of angles currently considered already suffices to describe the conformational motif of a P3AT chain by defining the orientation of the side chain and the orientation of each monomeric unit with respect to the following one. Adding two more parameters for the first two dihedral angles of a second alkyl chain would result in these authors' opinion in an unnecessary overcomplication of the subject.

Results and discussion

At first the torsion potential of a plain 2,2′-bithiophene (BT) molecule was computed, both to get a raw estimation of the magnitude of the thiophene–thiophene contribution to the overall torsion potential of a substituted BT, and to compare the performance of the MP2/6-311G(d,p) level of theory to other previously reported torsion potentials obtained by electron-correlated methods coupled with correlation-consistent bases.[16b,32] While the main characteristics of this potential energy curve are now well established thanks to various experimental evidence,[33–39] the reproduction of its shape by computational means in the last few decades underwent a path almost as long and tortuous as that of computational chemistry itself,[16b,32,40–51] spanning from early semiempirical approaches to highly-correlated first principles methods. Unfortunately, a clear trend has been unveiled by Duarte *et al.*[32] and successively confirmed by Raos *et al.*[16b] regarding the performance of MP2 with different bases. In fact, with an increasing number of base functions, co-planar transition states are found to lower significantly in energy, while the orthogonal ones rise slightly, minima remaining almost unchanged. Our torsion barrier (not reported) closely reproduces the one obtained by Duarte *et al.*[32] at the same level of theory, and is characterized by an overestimation of the energy barrier represented by the co-planar transition states and an underestimation of that of the orthogonal ones. This behaviour will also be present in the case of 3-alkyl-BTs, but, due to the steric hindrance of the alkyl group, it is expected to be of less relevance.

The theoretical potential energy curves of 3-hexyl-2,2′-bithiophene (HBT) are plotted against three different dihedral angles, namely θ, α, and β, as defined in Fig. 1. The nomenclature used to identify the angles and the various minimum energy conformers follows from that used for 3-hexylthiophene (3HT) in a previous report.[27] The three internal coordinates θ, α, and β represent, respectively, the reciprocal orientation of the two thiophene rings (T1 and T2 in Fig. 1), the tilting of the side chain (R1) relative to the thiophene ring it is attached to (T1), and the conformation of the first fragment of the side chain in its *syn–gauche–anti* arrangements. All torsion angles of the side chain beyond β will be set in all-*anti* conformation compatibly with P3AT packing requirements, and then relaxed. See ref. 27 for a more thorough discussion on this topic. For simplicity, θ and α will have the same sign (both positive or both negative) whenever the T2's sulphur atom and R1 are found on the same side of the T1's plane. It is worth noting that two isomers, respectively, characterized by the two triads of angles $\{\theta, \alpha, \beta\}$ and $\{-\theta, -\alpha, -\beta\}$ are specular to one another and share the same energy value. As a consequence, each couple of specular isomers will also share the same name for the purpose of this study. As for labelling of conformational isomers, in the case of 3-hexylthiophene four minimum energy conformations were identified and labelled with a roman numeral. In particular, **I** for the all-*anti* out-of-plane conformer, **II** for the all-*anti* in-plane conformer, **III** and **IV** for the two *gauche* out-of-plane arrangements. This very scheme will be used to identify the different configurations of the side chain, while the minimum energy arrangements of θ will be labelled with capital letters from **A** to **D**.

At an early stage, with the torsion barriers of BT and 3HT in mind, we assumed that a total of twelve minimum energy configurations would have been a realistic guess. The attachment of a side chain to BT would break symmetry and make its four-fold torsion potential curve actually consist of four non-equivalent minima. On the other hand, with T2 being free to rotate about the linking bond C–C, we assumed no **II**-like conformers would have been found, hence the twelve minima estimation. This is of course assuming steric interactions between R1 and T2 would not prevent any of these conformations from being observed, which is not likely to be valid in this case, making twelve a rather conservative esteem.

Fig. 2a shows the theoretical torsion barrier associated with the rotation of θ angle around the C–C bond linking T1 and T2. Each curve is obtained by optimizing the geometry and computing the energy of the molecule as a function of θ at different conformations of the side chain, which implied different values of β. As can be seen in Fig. 2c, which reports $\beta = f(\theta)$, all three configurations of the side chain (**I**, **III** and **IV**) are rather stable, as β does not change significantly along the whole range of variation of θ. On the other hand, the plot of $\alpha = f(\theta)$ in Fig. 2b shows that α is subject to large oscillations, allowing the system to adjust itself in order to accommodate for sterically unfavourable contacts, mostly from T2 and the first three methylenes of the side chain. Before proceeding with a detailed commentary, it should be made clear to the reader that the discontinuities found on the **IV** curves are due to the relaxation of all geometrical parameters but the focused dihedral angle, which may under certain conditions allow an internal coordinate to slip over a low-energy conformational transition state during the geometry optimization procedure, which means moving from a one-dimensional projection of the potential energy surface to another.

On the same curve, the minimum energy configurations on the spectrum of θ are labelled by a specific capital letter.

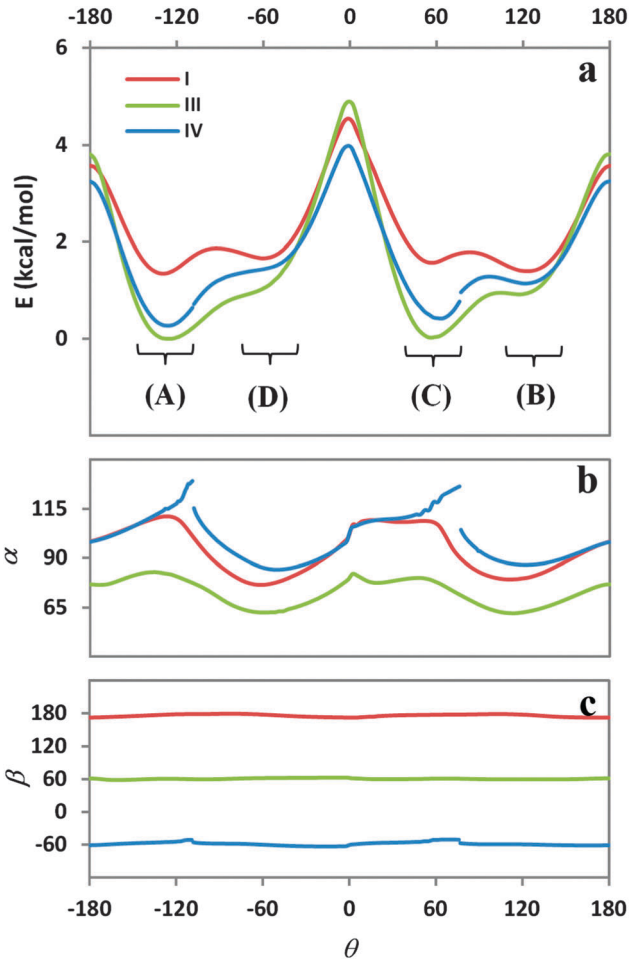

Fig. 2 Potential energy curves computed for HBT relative to θ angle (a) and the corresponding values of α (b) and β (c) angles. All angles are reported in degrees.

We chose arbitrarily to use **A** and **B** for the two transoid arrangements ($|\theta| > 90^\circ$) and **C** and **D** for the cisoid ones ($|\theta| < 90^\circ$). Although inappropriate, the *trans–cis* nomenclature has been often used to designate inter-ring conformations of conjugated molecules. Transoid–cisoid terming has thus been chosen in place of the *anti–syn* one for the inter-ring torsion angle θ in the present study, allowing for a more clear differentiation between inter-ring conformations and side chain arrangements (as the latter will be discussed using the appropriate *anti–syn* nomenclature). Among the three curves, these four values of θ are consistent with one another and also with the BT torsion potential, further confirming the existence of a well-defined set of favourable relative arrangements between T1 and T2. Interesting on this matter are the very low barriers (few tenths of a kcal mol^{-1}) corresponding to the orthogonal transition states, which make for an easy interconversion between **A**/**D** and **C**/**B** couples of minima. Observing the graph as a whole, an important consideration can be made regarding our initial guess: two minimum energy conformers are missing in the **D** position on the curves **III** and **IV**.

This is most likely due to excessive steric repulsion between the hydrogen atom in the 3′ position and the side chain. As already pointed out, the ruling steric interaction in HBT is in fact that of T2 with the first three methylene groups of the side chain R1, which makes the thiophene–thiophene interaction less important in comparison. With regard to the considerations made about BT at the beginning of this section, because the torsion barriers associated with co-planar configurations of HBT are more than an order of magnitude higher than those associated with the orthogonal ones, we expect the number of base functions used in the calculations to have a limited impact on the ratio between these two conformational transition state's energies.

With reference to the list of stable isomers gathered in Table 1, the minima on the curve **I** in Fig. 2a are all found within a range of 0.32 kcal mol^{-1}, with transoid conformations favoured over cisoid ones, similarly to what is observed for unsubstituted BT.[16b] On the other hand, the minima found on the two curves corresponding to *gauche* arrangements of the side chain, **III** and **IV**, are generally more stable than the corresponding *anti* ones (curve **I**), and do not follow the transoid *vs.* cisoid pattern. This is because the steric hindrance of a side chain in *gauche* conformation is larger than that in *anti* conformation, and dominates the torsion potential over the thiophene–thiophene interaction. In fact, the most stable **III**- and **IV**-like isomers are those which describe the same inter-planar angle $\Theta_1 = \theta_C = \theta_A + n \times 180^\circ$ ($n \in \mathbb{N}$) between T1 and T2, **A** and **C**, differing by about 180° to one another (refer to Table 1 for the actual values). The other *gauche* isomers (**B** and **D**) lie at a different T1–T2 inter-planar angle (Θ_2) and are generally less stable, again due to unfavourable interactions between R1 and T2. Indeed, this interaction hampers the flexibility of the molecule at a point that it prevents **III-D** and **IV-D** conformational isomers from being observed. The presence of these two inter-planar arrangements (Θ_1 and Θ_2) and the low orthogonal interconversion barriers between them plays a prominent role in the conformational freedom of HBT, and will affect almost every aspect of this study.

An important parameter to be considered in addition to torsion potentials for conjugated molecules is the length and stretching constant of the inter-ring bond. We report in Fig. 3 this T1–T2 distance as a function of θ for all three

Table 1 List of all stable isomers of HBT[a]

Isomer	E	α	β	θ
I-A	+1.34	111.0	177.8	−126.3
I-B	+1.40	80.2	177.8	126.5
I-C	+1.57	108.5	177.8	60.9
I-D	+1.66	76.6	178.2	−56.2
III-A	0.00	82.0	61.3	−123.7
III-B	+0.92	62.3	60.2	119.7
III-C	+0.02	78.8	61.4	58.2
IV-A	+0.27	115.2	−54.9	−123.7
IV-B	+1.14	86.6	−59.0	124.5
IV-C	+0.41	120.8	−50.2	64.1
V-A	+2.28	114.2	119.0	−106.1
V-C	+2.32	109.3	120.6	75.0

[a] MP2/6-311G(d,p) relative energies are reported in (kcal mol^{-1}). Angles are reported in degrees.

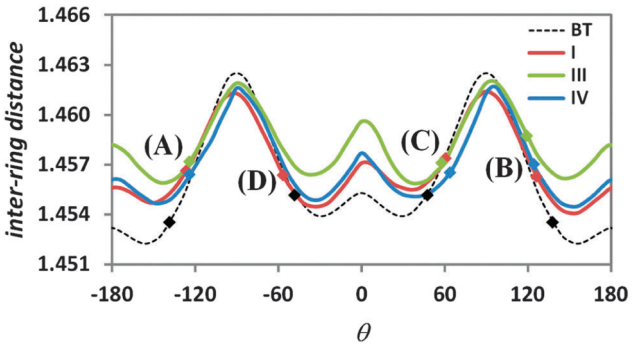

Fig. 3 Inter-ring distance (as the length of the bond linking T1 and T2) as a function of the inter-ring angle θ. Dots indicate minimum energy conformations for quick reference. Distances in Å, angles in degrees.

conformations of the side chain, and for unsubstituted bithiophene (BT). The inter-ring distance is larger for HBT, and is mostly consistent among all minima, the only exception being **III-B** with a slightly longer bond. This is in contrast to BT minima, which systematically differ between cisoid and transoid states. In addition, all three inter-ring distance profiles reported for HBT oscillate within a tighter range of values compared to BT. All these evidences further support the dominance of the side chain interaction with both thiophene rings over the thiophene–thiophene interaction itself (in both its electronic and steric contributions).

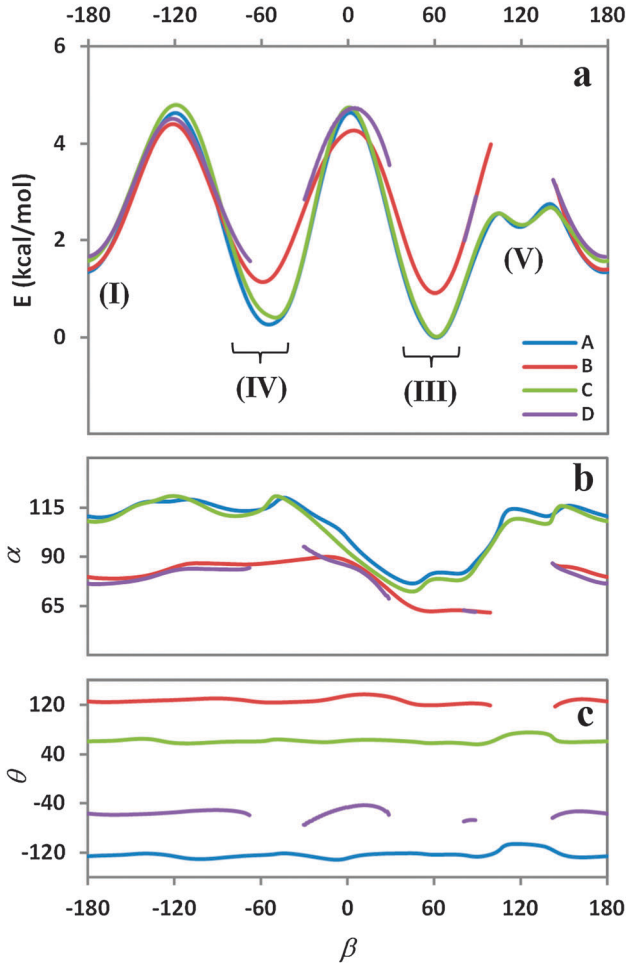

Fig. 4 Potential energy curves computed for HBT relative to β angle (a) and the corresponding values of α (b) and θ (c) angles. All angles are reported in degrees.

After reviewing the stable arrangements of β at different values of θ, stable arrangements of θ at different values of β will be now dealt with. In Fig. 4 the torsional barrier of HBT relative to the β angle is reported along with the corresponding plots of $\alpha = f(\beta)$ and $\theta = f(\beta)$. It is immediately evident that curves **A** and **C**, which share the same T1–T2 inter-planar arrangement Θ_1, show a very similar behaviour. Curves **B** and **D**, which share the other inter-planar arrangement Θ_2, also behave very similar to one another, but, unfortunately, the very low barriers of **A/D** and **C/B** interconversion already discussed make it difficult to obtain a converged result in certain regions of the β spectrum. This issue led to the ample blank regions visible in Fig. 4, where **B** and **D** curves fall, respectively, into the lower-energy wells of **C** and **A** curves. An interesting case on this matter is that of the missing fragments at $\beta = 120^\circ$ on curves **B** and **D**, which in turn are strictly bound to the behaviour of curves **A** and **C** in that same region. It is in fact very easy to spot the two minima labelled by the roman numeral **V** in the eclipsed region, where one would expect to find maximum energy points. Despite eclipsed conformations being usually not favoured in alkyl chains, an almost orthogonal arrangement of T1 and T2 allows in this case for a stabilizing interaction between several C–H bonds of the side chain and the π-cloud of T2.[52] It is not surprising at this point to notice that **V-A** and **V-C** describe the new T1–T2 inter-planar arrangement Θ_3, at, respectively, $\theta = -106.1^\circ$ and $\theta = 75.0^\circ$, about 180° apart from one another. It is now clear that in spite of the fact that thiophene is not as symmetric as say benzene, interacting alkyl moieties 'feel' its π-cloud and the steric repulsion it generates, but do not discriminate its orientation, hence the very similar relative energy of the conformers sharing the same T1–T2 inter-planar arrangement. It can also be noted that, similarly to the $\beta = f(\theta)$ plot of Fig. 2c, the $\theta = f(\beta)$ plot of Fig. 4c consists of nearly flat lines, which implies that the four arrangements of θ are well defined and are not heavily affected by the oscillations of β. The task of accommodating unfavourable steric contacts is delegated also in this case to α, which in Fig. 4b can be seen to vary roughly within the same range of values as in Fig. 2b.

The α angle, differently from θ and β, poses a somewhat ambiguous case. No α angle outside a range of $\pm(60:120)^\circ$ has been observed so far during the investigation of the other internal coordinates. The manipulation of this torsion angle is made difficult by the very low barriers of interconversion between **A/D** and **C/B** couples of minima, leading to regions in which transoid and cisoid conformers coexist and regions characterized by only one available θ conformation. Fig. 5a shows the theoretical potential curve associated with the torsion of α angle in the *anti* arrangement of the side chain. *Gauche* arrangements of the side chains are not displayed as the strain generated by the steric repulsion between R1 and T2 for

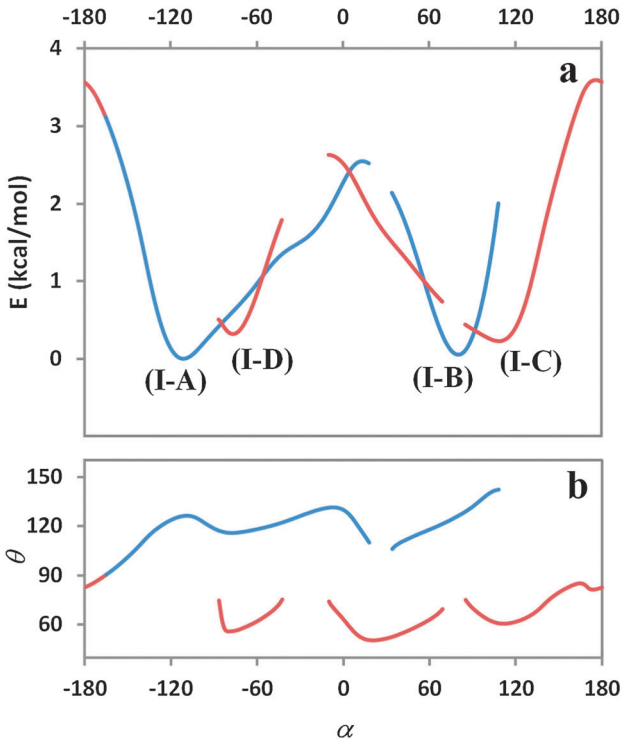

Fig. 5 Potential energy curve computed for HBT in conformation **I** of the side chain relative to the α angle (a), and the corresponding values of the θ angle (b). Segments corresponding to transoid and cisoid arrangements are represented in blue and red respectively. All angles are reported in degrees.

deviations of the α angle of only 10–15° from the optimum values listed in Table 1 (a much shorter range than the ±(60 : 120)° 'trust range' of the α angle itself) triggers a spurious transition of β to *anti* conformation. Fig. 5b plots the corresponding values of θ as a function of α. Several hiatuses, all characterized by values of the θ angle approaching the 90° mark, are present in Fig. 5a. This is because in this case the θ angle is in charge for what concerns the adjustment of bad steric contacts, and works around them by switching between transoid and cisoid arrangements. The relative stabilization of this switch is immediately noticeable in Fig. 5a by comparing the energy of the two at a given point on the horizontal axis. It is worth noting that the low **A/D** and **C/B** interconversion barriers in Fig. 2a refer to the transition from a minimum energy conformer to another, thus we can expect the same transition occurring between two non-equilibrium conformations to exploit even lower energy barriers, if at all. Another peculiar feature of the curve in Fig. 5a is the transoid–cisoid transition in the 180° region of α. In this configuration, the steric repulsion between R1 and T2 causes a strain able to assist the switch of θ from the transoid to the cisoid state and *vice versa* without any interruption, making it a rather spurious transition.

So far, twelve minimum energy conformations have been identified for 3-hexyl-2,2′-bithiophene. Four of them feature an *anti* arrangement of the side chain, six of them a *gauche* arrangement, and the last two a higher-energy eclipsed arrangement. In order to get a more complete perspective on the energy

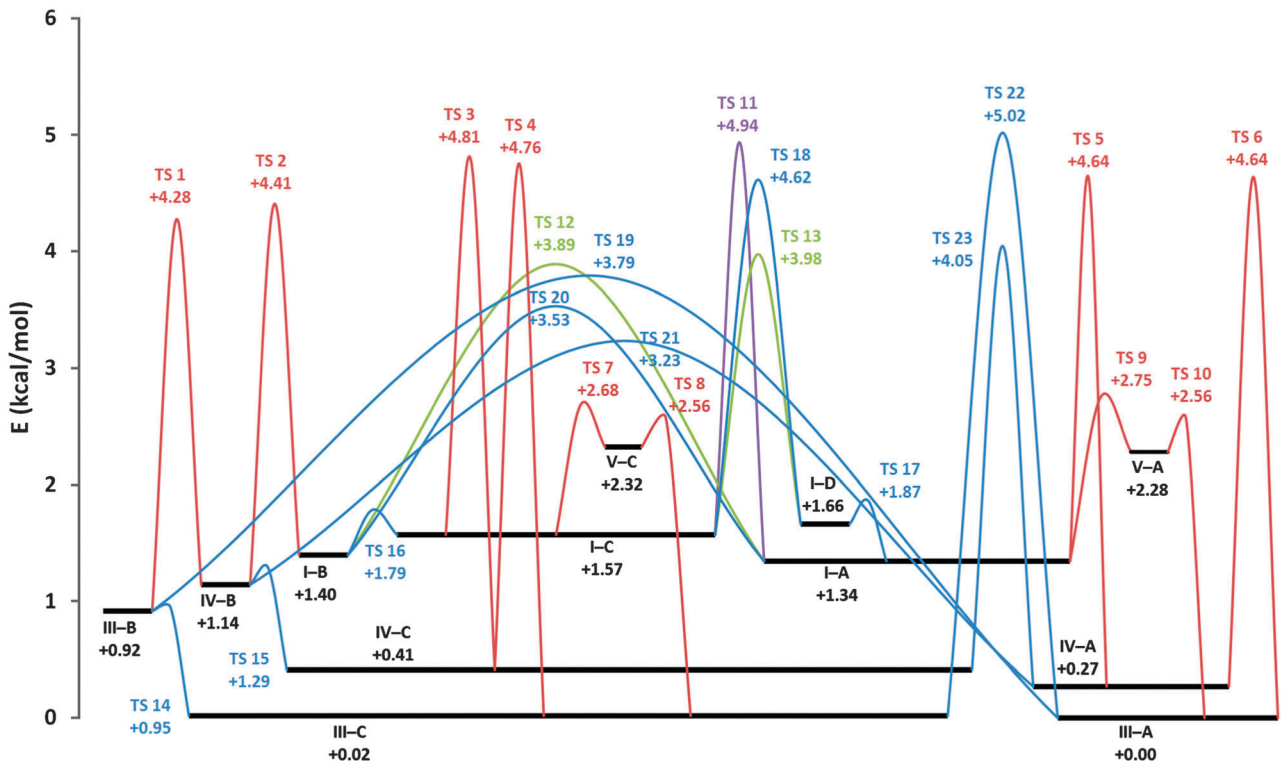

Fig. 6 Diagram summarizing the conformational freedom of HBT. Blue curves represent θ torsions, green curves represent α torsions, red ones β torsions. The purple curve presents a spurious transition involving both α and θ (see the text). Relative energies are reported in kcal mol^{-1}.

gaps that separate them, and on the energy barriers that instead connect them by the rotation of a single dihedral angle, all the torsion potential curves were merged in the diagram reported in Fig. 6. Minima are represented on an arbitrary energy axis, losing any geometrical information but the side chain arrangement (roman numerals) and the torsion angle associated with each transition. All conformers **III** and **IV**, characterized by a *gauche* arrangement of the side chain, are found to be more stable than *anti* ones, with eclipsed **V** isomers topping the series. Exchange/repulsion interactions and remote hyperconjugation phenomena between the side chain and both aromatic rings are at the origin of such energetic and conformational motifs. Folded side chains on conformers **III** and **IV** accomplish a high degree of stabilization due to a network of intramolecular CH–π interactions which are not present in conformers **I**.[27] Conformers **V** on the other hand, despite the folded geometries (similar to those of conformers **III**) encouraging extensive CH–π hyperconjugation, are governed by the strong repulsion between the eclipsed methylene groups.

Conformational transition states, numbered progressively from TS1 to TS23, vary substantially in energy (*e.g.* TS4 compared to TS14), but rarely exceed 5 kcal mol^{-1} on the relative axis. The isomer–isomer transitions with a lower energy barrier can be considered statistically more likely to occur than those exploiting a higher barrier. The lowest energy barriers reported in Fig. 6 represent the orthogonal transition states about the rotation of θ (TS14 through TS17), and the transition states leading eclipsed **V** conformers to the corresponding conformers **I** and **III**, prompted by the rotation of the β angle (TS7 through TS10). The isomer–isomer energy gaps associated with each of these eight conformational transitions amount to more than 80% of the corresponding barrier height when one or both isomers have **III**- or **IV**-like arrangements (TS14, TS15, TS8 and TS10), and to around 60% (except TS16 at 44%) for the remaining cases. Because the energy gap/barrier height ratios associated with all other conformational transitions settle well below 10%, such an imbalance for the aforementioned eight isomer–isomer transitions is expected to steadily favour the lowest energy isomer. The main practical effect of this observation is that conformers **B** and **D**, along with **V**-like ones, can be assumed to represent short-lived states of HBT, which is to say, T1–T2 inter-planar arrangements Θ_2 and Θ_3 are easily converted to Θ_1 arrangements without incurring in any relevant penalty. Nevertheless, these eight energy barriers are all found in a range of 1–4 times k_BT at room temperature (notably lower than a conformational transition in linear alkanes), most likely providing P3AT backbones with a high degree of flexibility.

In a realistic atomistic model of an amorphous P3HT region, we expect polymer chains to essentially consist of a series of monomer units featuring a more or less distorted version of one of the twelve $\{\theta, \alpha, \beta\}$ minimum energy triads of angles listed in Table 1, a few of which are expected to be rather short-lived as just mentioned. Intermolecular interactions with neighbouring chains may ultimately cause a systematic distortion of minima geometries from the isolated-molecule optimal configurations, but it is unlikely their role will be decisive, as stretching and compression of covalent bonds and angles usually dominate over noncovalent interactions in the assessment of minimum energy geometries, mainly because of the different orders of magnitude associated with the two phenomena. Moreover, intermolecular CH–π interactions between aromatic and aliphatic fragments[52] of adjacent chains are found to compete with their intramolecular counterparts. In fact, several tests performed on isolated P3HT hexamers at the ωB97X-D/6-311G(d,p)[53] level on a pruned 99 590 integration grid show that side chains in *gauche* arrangements **III** and **IV** can not only interact with T2, but can also easily interact with the thiophene ring beyond T2 provided the angle between them is adequate. One should however be careful when performing DFT calculations on larger systems, as the potential energy surface of a molecule may differ significantly over different computational methods. As an example, conformer **III-B** of HBT does not exist as a stable isomer at the ωB97X-D/6-311G(d,p) level of theory.

Worth noting is the existence on the potential energy surface of HBT of a few stable *gauche* isomers featuring a cisoid arrangement between T1 and T2, namely **III-C** and **IV-C**. This finding may expand our understanding of the chain-folded morphologies experimentally observed for P3ATs[54] and other alkylthiophene-based semiconducting materials such as PBTTT.[55] Chain-folding is a phenomenon in which a polymer chain exits and then re-enters a lamella. Because crystalline regions consist of ordered chains, the chain-folding segments are required to exit and re-enter the domain with a certain angle in order to avoid unnecessary mechanical strain, and have to connect two specific points on the domain surface, even more so in P3AT crystals due to the directionality of the polymer chains. Chain-folding in P3AT crystals is usually modelled as a sequence of *cis*-arranged monomer units, usually planar, whose actual count depends on the specific structural features of the polymer.[10c] It is controversial whether these chain-folds are completely randomized or are also ordered in an aligned fashion.[56] In a recent study[57] on a selection of thiophene-based semiconducting polymers, the abundance of different σ bond linkages along the backbone (*e.g.* head-to-tail junctions, head-to-thieno[3,2-*b*]thiophene junctions) was correlated with the experimental tendency of conjugated polymers to undergo extensive chain folding (methyl side chains were used in that circumstance). In spite of this, chain-folding phenomena are still commonly believed to take place during the growth process mostly due to entropic effects. The evidence of unexpectedly low-energy cisoid conformations in HBT suggests instead that chain-folding in the amorphous regions may be favoured also enthalpically over other random coil arrangements, or, at the very least, not enthalpically penalized.

It was mentioned in the Introduction that P3ATs form semicrystalline films, crystalline domains consisting of strongly π-stacked polythiophene chains separated by layers of aliphatic substituents. Single P3AT chains assume a trans-planar configuration in this phase, enhancing the conjugation of the unsaturated bonds, although a small deviation from co-planarity of thiophene rings is thought to be allowed at room

Table 2 List of all stable isomers of trans-planar HBT (θ = 180°)[a]

Isomer	E	α	β
I-P	+0.31	97.8	172.6
II-P	+2.04	0.0	180.0
III-P	+0.56	76.7	62.1
IV-P	0.00	97.7	−60.8

[a] MP2/6-311G(d,p) relative energies are reported in (kcal mol^{-1}). Angles are reported in degrees.

temperature.[58] Albeit not clearly evident, trans-planar configurations of HBT have already been described in this section. Such configurations represent in fact transition states on the potential energy surface of HBT, and can be seen both in Fig. 2a at $\theta = \pm 180°$ and in Fig. 6 as the θ-related isomer–isomer transitions labelled TS19, TS20, and TS21, respectively, characterized by a side chain in **III**, **I**, and **IV** arrangement. A new series of torsion potential curves was therefore computed on HBT as already done for the previously reported ones, this time forcing a trans-planar configuration of T1 and T2 rings by imposing a constant value of 180° for the θ angle. The series of trans-planar isomers was labelled with the capital letter **P**. Results are summarized in Table 2 and Fig. 7.

The torsional barrier associated with the rotation about the α angle of trans-planar HBT is shown in Fig. 7a along with that of trans-planar 3-methyl-2,2′-bithiophene (MBT), and that of 3-hexylthiophene (3HT) from ref. 27. In order to acquire a cleaner profile for HBT, its side chain was constrained to an all-staggered arrangement at this stage, because otherwise a twisting motion to *gauche* conformations of the β angle begins to be noticeable beyond values of α of around ±120°. MBT is reported here as an example of a system commonly used to economize on the simulation of inter-ring torsion potentials of P3ATs with longer side chains. Another example of a common substitute would be trans-planar 3-ethyl-2,2′-bithiophene, which in this case behaves much similarly to HBT. Unfortunately, neither methyl- nor ethyl-substituted bithiophenes can produce any **III**- or **IV**-like *gauche* conformation of the side chain, and should in general be avoided.

With reference to Fig. 7a, it is immediately evident the three reported profiles behave differently to one another in many ways. First of all, there is an order of magnitude between the energy barriers' height obtained for HBT and those obtained for MBT and 3HT. Moreover, because of the strong steric repulsion between T2 and R1 (which is obviously not present in 3HT), the main planar isomers of HBT and MBT are found at $\alpha = 0°$, whereas at $\alpha = \pm 180°$ a high-energy relative minima and a conformational transition state, respectively, are found. It is interesting at this point to focus on the non-planar minima. MBT out-of-plane minima lie at $\alpha = \pm 120°$ because of their symmetric 3-fold torsion barrier. 3HT and MBT out-of-plane minima on the other hand are found, respectively, at around $\alpha = \pm 75°$ and $\alpha = \pm 96°$, the former in the typical region of **III**-like *gauche* conformers and the latter in the region of **IV**-like ones. This observation anticipates the main difference between the torsion potentials of HBT and 3HT associated with the rotation

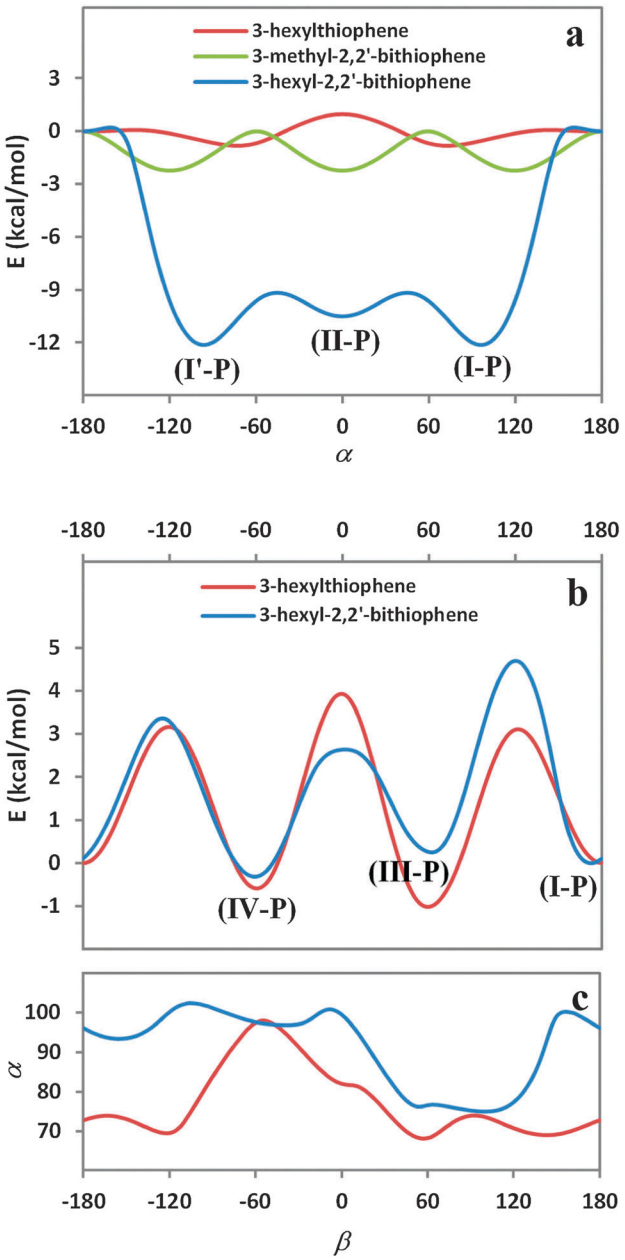

Fig. 7 Potential energy curves computed for trans-planar HBT (θ = 180°) relative to α (a) and β angles (b), and the values of the former as a function of the latter (c). The same curves computed for MBT and 3HT are also shown for comparison when appropriate. All angles are reported in degrees.

about the β angle, reported in Fig. 7b. In this case, because of the strong repulsion between T2 and R1, **III**-like conformations of the side chains cause more strain than **I**-like arrangements, resulting in the prevalence of **IV**-like ones in HBT. This statement is further corroborated by the $\alpha = f(\beta)$ plot of Fig. 7c, which shows that the α angle of HBT, when relaxed, oscillates between 93° and 103° for the most part of the β spectrum, shifting to the 75–77° region only for arrangements of the β angle typical of **III**-like isomers, as completely opposed to what has been observed for 3HT.[27]

Trans-planar arrangements **I-P**, **III-P** and **IV-P** of isolated HBT are all inherently found more than 3 kcal mol^{-1} higher in energy compared to non-planar isomers, but this is due to the absence of neighbouring chains. Within the semicrystalline bulk of thin films, the stabilizing intermolecular interactions between planar self-assembled layers outdo the non-specific interactions between non-planar backbones in the amorphous phase. Indeed, a temporary, slight loss of co-planarity would not result in major enthalpic penalties as far as π-stacking is concerned, while allowing for a more comfortable transition between different side chain arrangements. Moreover, the level of theory employed for this investigation has been reported to overestimate the energy of co-planar transition states in bithiophene,[16b,32] so that the 'toll' for co-planarity may not be as high as depicted in this report. In order to fully appreciate the magnitude of such complex morphological changes, the chemical environment of the polymer chains must be modelled explicitly to some extent.

Concluding remarks

In the present study, the conformational stability of a monosubstituted bithiophene molecule was investigated through first principles quantum mechanical means in order to provide better insights into the intrinsic flexibility of regioregular poly(3-alkylthiophenes)' chains. Both fully-relaxed and trans-conjugated arrangements were taken into account, modelling polymer chains within the amorphous interlamellar environment and within the limit-ordered crystalline domains, respectively. The aliphatic substituent is found to play a non-negligible role in the energetic and geometrical aspects of bithiophene. All the conformational motifs discussed herein can be extended to other polymeric materials containing an alkylthiophene unit connected in position 2 to a generic aromatic ring, as no evidence of specific interactions involving sulphur atoms was detected. The salient conclusions drawn from this study follow.

(1) The inter-ring torsion potential of isomers of 3-alkyl-2,2′-bithiophene characterized by a side chain in *anti* arrangement is similar to that of unsubstituted 2,2′-bithiophene, *i.e.* dominated by thiophene–thiophene interactions favouring transoid over cisoid configurations. Instead, folded side chains (with the β angle in a *gauche* conformation) interact strongly with the adjacent thiophene ring, resulting in a set of homologous transoid–cisoid couples of isomers whose energetic aspects are ultimately determined by the angle between the planes described by the two aromatic rings (at $\theta + n \times 180^\circ$, $n \in \mathbb{N}$) regardless of the specific orientation.

(2) Isomers with folded side chains are generally more stable than isomers with extended side chains. This is due to a network of CH–π hydrogen-bond-like intramolecular interactions between the methylene groups of the side chain and the π electrons of thiophene rings.

(3) Surprisingly stable isomers with a cisoid (non-planar) inter-ring configuration do exist, suggesting that chain-folding phenomena at the surface of crystalline domains of P3HT are not as much enthalpically penalized as they are commonly thought to be.

(4) As observed from gas phase calculations on a series of $(3HT)_n$ oligomers, intramolecular CH–π interactions within each polymer chain may effectively compete with intermolecular CH–π interactions with neighbouring chains. In particular, extended side chains favour intermolecular interactions and give rise to transoid-arranged sequences of consecutive monomers, mostly, while folded side chains promote auto-interaction and give mostly rise to cisoid-arranged sequences.

(5) Constrained trans-planar inter-ring configurations of 3-alkyl-2,2′-bithiophene have been used to model conjugated chains within the crystalline domains. In these circumstances, side chain energetics are found to be dominated by the strong repulsive interaction with the hydrogen atom in the 3′ position. As a consequence, the least strained arrangements of the side chain lie within a tight range of values of $98 \pm 5^\circ$ on the α spectrum. This makes folded **IV**-like and fully-extended **I**-like conformations the most favourable.

Acknowledgements

This work has been supported by Regione Lombardia and CILEA Consortium through a LISA Initiative (Laboratory for Interdisciplinary Advanced Simulation) 2011 grant.

Notes and references

1 (*a*) F. So, *Organic Electronics: Materials, Processing, Devices and Applications*, CRC, Boca Raton, FL, 2009; (*b*) W. S. Wong and A. Salleo, *Flexible Electronics: Materials and Applications*, Springer-Verlag, Berlin, 2009.

2 (*a*) N. S. Sariciftci, L. Smilowitz, A. J. Heeger and F. Wud, *Science*, 1992, **5087**, 1474–1476; (*b*) H. Sirringhaus, P. J. Brown, R. H. Friend, M. M. Nielsen, K. Bechgaard, B. M. W. Langeveld-Voss, A. J. H. Spiering, R. A. J. Janssen, E. W. Meijer, P. Herwig and D. M. de Leeuw, *Nature*, 1999, **401**, 685–688; (*c*) H. Sirringhaus, N. Tessler and R. H. Friend, *Science*, 1998, **5370**, 1741–1744; (*d*) H. Sirringhaus, N. Tessler, D. S. Thomas, P. J. Brown and R. H. Friend, *Adv. Solid State Phys.*, 1999, **39**, 101–110.

3 (*a*) H. Hoppe and N. S. Sariciftci, *J. Mater. Res.*, 2004, **19**, 1924–1945; (*b*) K. M. Coakley and M. D. McGehee, *Chem. Mater.*, 2004, **16**, 4533–4542; (*c*) S. Günes, H. Neugebauer and N. S. Sariciftci, *Chem. Rev.*, 2007, **107**, 1324–1338; (*d*) T. M. Clarke and J. R. Durrant, *Chem. Rev.*, 2010, **110**, 6736–6767.

4 (*a*) C. J. Brabec, N. S. Sariciftci and J. C. Hummelen, *Adv. Funct. Mater.*, 2001, **11**, 15–26; (*b*) S. Gunes and N. S. Sariciftci, *Inorg. Chim. Acta*, 2008, **361**, 581–588; (*c*) C. Y. Ma, X. Gong, K. Lee and A. Heeger, *Adv. Funct. Mater.*, 2005, **15**, 1617–1622; (*d*) R. Mauer, M. Kastler and F. Laquai, *Adv. Funct. Mater.*, 2010, **20**, 2085–2092; (*e*) S.-H. Lee, D.-H. Kim, G.-S. Lee and J.-G. Park, *J. Phys. Chem. C*, 2009, **113**, 21915–21920; (*f*) M. T. Dang, L. Hirsch and

G. Wantz, *Adv. Mater.*, 2011, **23**, 3597–3602; (*g*) M. Al-Ibrahim, O. Ambacher, S. Sensfuss and G. Gobsch, *Appl. Phys. Lett.*, 2005, **86**, 201120.

5 (*a*) F. Garnier, Field-Effect Transistors Based on Conjugated Materials, in *Electronic Materials: The Oligomer Approach*, ed. K. Müllen and G. Wegner, Wiley-VCH, Weinheim, 1998; (*b*) H. Sirringhaus, *Adv. Mater.*, 2005, **17**, 2411–2425; (*c*) J. Y. Kim, K. Lee, N. E. Coates, D. Moses, T.-Q. Nguyen, M. Dante and A. J. Heeger, *Science*, 2007, **317**, 222–225; (*d*) R. J. Kline, D. M. DeLongchamp, D. A. Fischer, E. K. Lin, L. J. Richter, M. L. Chabinyc, M. F. Toney, M. Heeney and I. McCulloch, *Macromolecules*, 2007, **40**, 7960–7965; (*e*) Y. D. Park, D. H. Kim, Y. Jang, J. H. Cho, M. Hwang, H. S. Lee, J. A. Lim and K. Cho, *Org. Electron.*, 2006, **7**, 514–520; (*f*) W. D. Oosterbaan, J. C. Bolsee, A. Gadisa, V. Vrindts, S. Bertho, J. D'Haen, T. J. Cleij, L. Lutsen, C. R. McNeill, L. Thomsen, J. V. Manca and D. Vanderzande, *Adv. Funct. Mater.*, 2010, **20**, 792–802.

6 (*a*) X. M. Jiang, R. Osterbacka, O. Korovyanko, C. P. An, B. Horovitz, R. A. J. Janssen and Z. V. Vardeny, *Adv. Funct. Mater.*, 2002, **12**, 587–597; (*b*) R. Mauer, M. Kastler and F. Laquai, *Adv. Funct. Mater.*, 2010, **20**, 2085–2092; (*c*) Y. Kim, S. Cook, S. M. Tuladhar, S. A. Choulis, J. Nelson, J. R. Durrant, D. D. C. Bradley, M. Giles, I. Mcculloch, C. S. Ha and M. A. Ree, *Nat. Mater.*, 2006, **5**, 197–203; (*d*) K. Tajima, Y. Suzuki and K. Hashimoto, *J. Phys. Chem. C*, 2008, **112**, 8507–8510; (*e*) Y. Suzuki, K. Hashimoto and K. Tajima, *Macromolecules*, 2007, **40**, 6521–6528; (*f*) P. J. Brown, D. S. Thomas, A. Kohler, J. S. Wilson, J. S. Kim, C. M. Ramsdale, H. Sirringhaus and R. H. Friend, *Phys. Rev. B: Condens. Matter Mater. Phys.*, 2003, **67**, 064203.

7 (*a*) M. J. Winokur, P. Wamsely, J. Moulton, P. Smith and A. J. Heeger, *Macromolecules*, 1991, **24**, 3812–3815; (*b*) K. Tashiro, K. Ono, Y. Minagawa, M. Kobayashi, T. Kawai and K. Yoshino, *J. Polym. Sci., Part B: Polym. Phys.*, 1991, **29**, 1223–1233; (*c*) J. Mardalen, E. J. Samuelsen, O. R. Gautun and P. H. Carsen, *Solid State Commun.*, 1991, **77**, 337–339; (*d*) G. Gustafsson, O. Iganas, H. Osterholm and J. Laakso, *Polymer*, 1991, **32**, 1574–1580; (*e*) J. Mardalen, E. J. Samuelsen, O. R. Gautun and P. H. Carsen, *Synth. Met.*, 1992, **48**, 363–380.

8 (*a*) T. J. Prosa, M. J. Winokur, J. Moulton, P. Smith and A. J. Heeger, *Macromolecules*, 1992, **25**, 4364–4372; (*b*) T. J. Prosa, M. J. Winokur, J. Moulton and P. Smith, *Synth. Met.*, 1993, **55**, 370–377; (*c*) K. Tashiro, M. Kobayashi, S. Morito, T. Kawai and K. Yoshino, *Synth. Met.*, 1995, **69**, 397–398; (*d*) A. Bolognesi, W. Porzio, F. Provasoli and T. Ezquerra, *Makromol. Chem.*, 1993, **194**, 817–827; (*e*) T. J. Prosa, M. J. Winokur and R. D. McCullough, *Macromolecules*, 1996, **29**, 3654–3656; (*f*) S. V. Meille, V. Romita, T. Caronna, A. Lovinger, M. Catellani and L. Belobrzeckaja, *Macromolecules*, 1997, **30**, 7898–7905.

9 (*a*) S. Malik and A. K. Nandi, *J. Polym. Sci., Part B: Polym. Phys.*, 2002, **40**, 2073–2085; (*b*) R. J. Kline, M. D. McGehee, E. N. Kadnikova, J. Liu and J. M. J. Fréchet, *Adv. Mater.*, 2003, **18**, 1519–1522; (*c*) V. Causin, C. Marega, A. Marigo, L. Valentini and J. M. Kenny, *Macromolecules*, 2005, **38**, 409–415; (*d*) A. Zen, M. Saphiannikova, D. Neher, J. Grenzer, S. Grigorian, U. Pietsch, U. Asawapirom, S. Janietz, U. Scherf, I. Lieberwirth and G. Wegner, *Macromolecules*, 2006, **39**, 2162–2171; (*e*) R. Zhang, B. Li, M. C. Iovu, M. Jeffries-EL, G. Sauvé, J. Cooper, S. Jia, S. Tristram-Nagle, D. M. Smilgies, D. N. Lambeth, R. D. McCullough and T. Kowalewski, *J. Am. Chem. Soc.*, 2006, **128**, 3480–3481; (*f*) M. Brinkmann and P. Rannou, *Adv. Funct. Mater.*, 2007, **17**, 101–108.

10 (*a*) M. Catellani, S. Luzzati, F. Bertini, A. Bolognesi, F. Lebon, G. Longhi, S. Abbate, A. Famulari and S. V. Meille, *Chem. Mater.*, 2002, **14**, 4819–4826; (*b*) P. Arosio, A. Famulari, M. Catellani, S. Luzzati, L. Torsi and S. V. Meille, *Macromolecules*, 2007, **40**, 3–5; (*c*) P. Arosio, A. Famulari, M. Moreno, G. Raos, M. Catellani and S. V. Meille, *Chem. Mater.*, 2009, **21**, 78–87; (*d*) N. Kayunkid, S. Uttiya and M. Brinkmann, *Macromolecules*, 2010, **43**, 4961–4967.

11 (*a*) T. S. Shabi, S. Grigorian, M. Brinkmann, U. Pietsch, N. Koenen, N. Kayunkid and U. Scherf, *J. Appl. Polym. Sci.*, 2012, **125**, 2335–2341; (*b*) H. Yang, S. W. Lefevre, C. Y. Ryu and Z. Bao, *Appl. Phys. Lett.*, 2007, **90**, 172116; (*c*) A. Salleo, R. J. Kline, D. M. DeLongchamp and M. L. Chabinyc, *Adv. Mater.*, 2010, **22**, 3812–3838; (*d*) M. Brinkmann and J. C. Wittmann, *Adv. Mater.*, 2006, **18**, 860–863.

12 (*a*) W. R. Salaneck, O. Inganäs, B. Thémans, J. O. Nilsson, B. Sjögren, J. E. Österholm, J. L. Brédas and S. Svensson, *J. Chem. Phys.*, 1988, **89**, 4613–4620; (*b*) M. J. Winokur and W. Chunwachirasiri, *J. Polym. Sci., Part B: Polym. Phys.*, 2003, **41**, 2630–2648.

13 C. McNeill, *J. Polym. Sci., Part B: Polym. Phys.*, 2011, **49**, 909–919.

14 (*a*) K. Do, D. M. Huang, R. Faller and A. J. Moule, *Phys. Chem. Chem. Phys.*, 2010, **12**, 14735–14739; (*b*) D. M. Huang, R. Faller, K. Do and A. J. Moule, *J. Chem. Theory Comput.*, 2010, **6**, 526–537; (*c*) D. M. Huang, A. J. Moule and R. Faller, *Fluid Phase Equilib.*, 2011, **302**, 21–25; (*d*) D. L. Cheung, D. P. McMahon and A. Troisi, *J. Phys. Chem. B*, 2009, **113**, 9393–9401; (*e*) S. Dag and L.-W. Wang, *J. Phys. Chem. B*, 2010, **114**, 5997–6000; (*f*) Y.-K. Lan and C.-I. Huang, *J. Phys. Chem. B*, 2008, **112**, 14857–14862; (*g*) Y.-K. Lan, C. H. Yang and H.-C. Yang, *Polym. Int.*, 2010, **59**, 16–21.

15 (*a*) C. Melis, L. Colombo and A. Mattoni, *J. Phys. Chem. C*, 2011, **115**, 576–581; (*b*) D. P. McMahon, D. L. Cheung and A. Troisi, *J. Phys. Chem. Lett.*, 2011, **2**, 2737–2741; (*c*) A. Famulari, G. Raos, A. Baggioli, M. Casalegno, R. Po and S. V. Meille, *J. Phys. Chem. B*, 2012, **116**, 14504–14509; (*d*) S. Hirata, *Phys. Chem. Chem. Phys.*, 2009, **11**, 8397–8412; (*e*) D. L. Cheung and A. Troisi, *Phys. Chem. Chem. Phys.*, 2008, **10**, 5941–5952; (*f*) D. L. Cheung, D. P. McMahon and A. Troisi, *J. Am. Chem. Soc.*, 2009, **131**, 11179–11186.

16 (*a*) R. S. Bhatta, Y. Y. Yimer, M. Tsige and D. S. Perry, *Comput. Theor. Chem.*, 2012, **995**, 36–42; (*b*) G. Raos, A. Famulari and V. Marcon, *Chem. Phys. Lett.*, 2003, **379**, 364–372.

17 W. Kohn and L. J. Sham, *Phys. Rev.*, 1965, **140**, A1133.

18 M. J. S. Dewar and W. Thiel, *J. Am. Chem. Soc.*, 1977, **99**, 4899–4907.

19 (*a*) J. J. P. Stewart, *J. Comput. Chem.*, 1989, **10**, 209–220; (*b*) J. J. P. Stewart, *J. Mol. Model.*, 2007, **13**, 1173–1213.

20 J. A. Pople, D. P. Santry and G. A. Segal, *J. Chem. Phys.*, 1965, **43**, S130.

21 A. R. Leach, *Molecular Modelling. Principles and Applications*, Pearson Education Limited, Harlow, England, 2001.

22 (*a*) R. J. Bartlett and G. D. Purvis III, *Int. J. Quantum Chem.*, 1978, **14**, 561–581; (*b*) J. A. Pople, R. Krishnan, H. B. Schlegel and J. S. Binkley, *Int. J. Quantum Chem.*, 1978, **14**, 545–560; (*c*) G. D. Purvis III and R. J. Bartlett, *J. Chem. Phys.*, 1982, **76**, 1910–1918; (*d*) J. A. Pople, M. Head-Gordon and K. Raghavachari, *J. Chem. Phys.*, 1987, **87**, 5968–5975; (*e*) G. E. Scuseria, C. L. Janssen and H. F. Schaefer III, *J. Chem. Phys.*, 1988, **89**, 7382–7387.

23 The actual size limits for a 'small', 'medium' or 'large' system are rather difficult to define. The functional forms commonly used to describe molecular mechanics potentials are relatively simple, and only depend on the position of the nuclei, which is known at every iteration. Each contribution can thus be computed independently, and, provided enough computational resources, even simultaneously. Molecular mechanics simulations benefit greatly from any level of parallelization, so that terms such as 'small system' and 'large system', on top of changing their meaning in time due to hardware technological advances, also depend on the amount of computational resources available.

24 *Reviews in Computational Chemistry*, ed. K. B. Lipkowitz and D. B. Boyd, VCH Publishers, New York, 1990.

25 (*a*) A. Maillard and A. Rochefort, *Phys. Rev. B: Condens. Matter Mater. Phys.*, 2009, **79**, 115207; (*b*) J. E. Northrup, *Phys. Rev. B: Condens. Matter Mater. Phys.*, 2007, **76**, 245202; (*c*) K. H. DuBay, M. L. Hall, T. F. Hughes, C. Wu, D. R. Reichman and R. A. Friesner, *J. Chem. Theory Comput.*, 2012, **8**, 4556–4569; (*d*) R. Colle, G. Grosso, A. Ronzani and C. M. Zicovich-Wilson, *Phys. Status Solidi B*, 2011, **248**, 1360–1368.

26 (*a*) G. Raos, A. Famulari, S. V. Meille, M. C. Gallazzi and G. Allegra, *J. Phys. Chem. A*, 2004, **108**, 691–698; (*b*) M. Moreno, M. Casalegno, G. Raos, S. V. Meille and R. Po, *J. Phys. Chem. B*, 2010, **114**, 1591–1602; (*c*) M. Casalegno, A. Baggioli, A. Famulari, S. V. Meille, T. Nicolini, R. Po and G. Raos, *EPJ Web Conf.*, 2012, **33**, 02002.

27 A. Baggioli, S. V. Meille, G. Raos, R. Po, M. Brinkmann and A. Famulari, *Int. J. Quantum Chem.*, 2013, **113**, 2154–2162.

28 (*a*) C. Møller and M. S. Plesset, *Phys. Rev.*, 1934, **46**, 618–622; (*b*) M. Head-Gordon, J. A. Pople and M. J. Frisch, *Chem. Phys. Lett.*, 1988, **153**, 503–506; (*c*) S. Sæbø and J. Almlöf, *Chem. Phys. Lett.*, 1989, **154**, 83–89; (*d*) M. J. Frisch, M. Head-Gordon and J. A. Pople, *Chem. Phys. Lett.*, 1990, **166**, 275–280; (*e*) M. J. Frisch, M. Head-Gordon and J. A. Pople, *Chem. Phys. Lett.*, 1990, **166**, 281–289; (*f*) M. Head-Gordon and T. Head-Gordon, *Chem. Phys. Lett.*, 1994, **220**, 122–128.

29 (*a*) R. Krishnan, J. S. Binkley, R. Seeger and J. A. Pople, *J. Chem. Phys.*, 1980, **72**, 650–654; (*b*) A. D. McLean and G. S. Chandler, *J. Chem. Phys.*, 1980, **72**, 5639–5648; (*c*) M. J. Frisch, J. A. Pople and J. S. Binkley, *J. Chem. Phys.*, 1984, **80**, 3265–3269.

30 M. J. Frisch, G. W. Trucks, H. B. Schlegel, G. E. Scuseria, M. A. Robb, J. R. Cheeseman, G. Scalmani, V. Barone, B. Mennucci, G. A. Petersson, H. Nakatsuji, M. Caricato, X. Li, H. P. Hratchian, A. F. Izmaylov, J. Bloino, G. Zheng, J. L. Sonnenberg, M. Hada, M. Ehara, K. Toyota, R. Fukuda, J. Hasegawa, M. Ishida, T. Nakajima, Y. Honda, O. Kitao, H. Nakai, T. Vreven, J. A. Montgomery, Jr., J. E. Peralta, F. Ogliaro, M. Bearpark, J. J. Heyd, E. Brothers, K. N. Kudin, V. N. Staroverov, R. Kobayashi, J. Normand, K. Raghavachari, A. Rendell, J. C. Burant, S. S. Iyengar, J. Tomasi, M. Cossi, N. Rega, J. M. Millam, M. Klene, J. E. Knox, J. B. Cross, V. Bakken, C. Adamo, J. Jaramillo, R. Gomperts, R. E. Stratmann, O. Yazyev, A. J. Austin, R. Cammi, C. Pomelli, J. W. Ochterski, R. L. Martin, K. Morokuma, V. G. Zakrzewski, G. A. Voth, P. Salvador, J. J. Dannenberg, S. Dapprich, A. D. Daniels, Ö. Farkas, J. B. Foresman, J. V. Ortiz, J. Cioslowski and D. J. Fox, *Gaussian 09 Revision C.01*, Gaussian, Inc., Wallingford, CT, 2009.

31 (*a*) S. F. Boys and F. Bernanrdi, *Mol. Phys.*, 1970, **19**, 553–566; (*b*) A. Famulari, E. Gianinetti, M. Raimondi and M. Sironi, *Int. J. Quantum Chem.*, 1998, **69**, 151–158; (*c*) M. Sironi and A. Famulari, *Theor. Chem. Acc.*, 2000, **103**, 417–422; (*d*) D. Asturiol, M. Duran and P. Salvador, *J. Chem. Phys.*, 2008, **128**, 144108; (*e*) R. M. Balabin, *J. Chem. Phys.*, 2008, **129**, 164101.

32 H. A. Duarte, H. F. Dos Santos, W. R. Rocha and W. B. De Almeida, *J. Chem. Phys.*, 2000, **113**, 4206–4215.

33 A. Almenningen, O. Bastiansen and P. Svendås, *Acta Chem. Scand.*, 1958, **12**, 1671–1674.

34 P. Bucci, M. Longeri, C. A. Veracini and L. Lunazzi, *J. Am. Chem. Soc.*, 1974, **96**, 1305–1309.

35 L. C. Ter Beek, D. S. Zimmerman and E. E. Burnell, *Mol. Phys.*, 1991, **74**, 1027–1035.

36 S. Samdal, E. J. Samulsen and H. V. Volden, *Synth. Met.*, 1993, **59**, 259–265.

37 M. Takayanagi, T. Gejo and I. Hanazaki, *J. Phys. Chem.*, 1994, **98**, 12893–12898.

38 J. E. Chadwick and B. E. Kohler, *J. Phys. Chem.*, 1994, **98**, 3631–3637.

39 R. Bernardi, F. Spinozzi and C. Zannoni, *Liq. Cryst.*, 1994, **16**, 381–397.

40 (*a*) J. L. Brédas, G. B. Street, B. Thémans and J. M. André, *J. Chem. Phys.*, 1985, **83**, 1323–1329; (*b*) J. L. Brédas, B. Thémans, J. M. André, A. J. Heeger and F. Wudl, *Synth. Met.*, 1985, **11**, 343–352.

41 U. Nagashima, H. Fujimoto and D. H. Inokuchi, *J. Mol. Struct.*, 1989, **197**, 265–289.

42 L. Navarrete, B. Tian and G. Zerbi, *Synth. Met.*, 1990, **38**, 299–312.

43 G. Distefano, M. Dal Colle, D. Jones, M. Zambianchi, L. Favaretto and A. Modelli, *J. Phys. Chem.*, 1993, **97**, 3504–3509.

44 C. Quattrocchi, R. Lazzaroni and J. L. Brédas, *Chem. Phys. Lett.*, 1993, **208**, 120–124.

45 M. Belletête, M. Leclerc and G. Durocher, *J. Phys. Chem.*, 1994, **98**, 9450–9456.
46 V. Hernandez and J. T. Lopez Navarrete, *J. Chem. Phys.*, 1994, **101**, 1369–1377.
47 E. Ortí, P. M. Viruela, J. Sánchez-Marín and F. Tomás, *J. Phys. Chem.*, 1995, **99**, 4955–4963.
48 M. Belletête, N. Di César, M. Leclerc and G. Durocher, *Chem. Phys. Lett.*, 1996, **250**, 31–39.
49 P. Viruela, R. Viruela and E. Ortí, *Int. J. Quantum Chem.*, 1998, **70**, 303–312.
50 A. Karpfen, C. H. Choi and M. Kertesz, *J. Phys. Chem. A*, 1997, **101**, 7426–7433.
51 N. Di César, M. Belletête, M. Leclerc and G. Durocher, *Synth. Met.*, 1998, **94**, 291–298.
52 (*a*) M. Nishio, M. Hirota and Y. Umezawa, *The CH/π interaction: Evidence, Nature, and Consequencies*, Wiley-VCH, New York, 1998; (*b*) K. E. Riley, M. Pitoňák, P. Jurečka and P. Hobza, *Chem. Rev.*, 2010, **110**, 5023–5063; (*c*) P. Hobza and Z. Havlas, *Chem. Rev.*, 2000, **100**, 4253–4264.
53 (*a*) J.-D. Chai and M. Head-Gordon, *Phys. Chem. Chem. Phys.*, 2008, **10**, 6615–6620; (*b*) J.-D. Chai and M. Head-Gordon, *J. Chem. Phys.*, 2008, **128**, 084106.
54 E. Mena-Osteritz, A. Meyer, B. M. V. Langeveld-Voss, R. A. J. Janssen, E. W. Meijer and P. Bauerle, *Angew. Chem., Int. Ed.*, 2000, **39**, 2680–2684.
55 I. McCulloch, M. Heeney, C. Bailey, K. Genevicius, I. MacDonald, M. Shkunov, D. Sparrowe, S. Tierney, R. Wagner, W. Zhang, M. L. Chabinyc, R. J. Kline, M. D. McGehee and M. F. Toney, *Nat. Mater.*, 2006, **5**, 328–333.
56 (*a*) D. C. Bassett, *Principles of Polymer Morphology*, Cambridge University Press, 1981; (*b*) L. Mandelkern, *Crystallization of Polymers: Volume 1, Equilibrium Concepts*, Cambridge University Press, 2004.
57 J. Liu, I. A. Mikhaylov, J. Zou, I. Osaka, A. E. Masunov, R. D. McCullough and L. Zhai, *Polymer*, 2011, **52**, 2302–2309.
58 J.-L. Fave, *Excitons in Chains of Thiophene Rings*, Springer Series in Solid-State Sciences, 1992, vol. 107, pp. 60–62.